4.1 Introduction

One of the most important biochemical molecules in the vitamin family is ascorbic acid (AA), which plays a key role in many biological processes, including the inhibition and prevention of cancer as well as the scavenging of free radicals [Navadeepthy et al., 2020; Dhara et al., 2019; Song et al., 2016; He et al., 2017; Santhanam et al., 1961; Sapner et al., 2021]. Unfortunately, the human body cannot produce AA, so daily diet supplements are the only source to complete such needs. The standard range of AA in a healthy life is laying between 0.6- 2 mg dL^{-1}. However, disturbance in their concentration can cause various complications like stomach pain, muscle pain, and diseases [Dhara et al., 2019]. Thus, a regular diagnosis of AA content becomes paramount for a fair and healthy body and receives unconditional worldwide attention. In this connection, various techniques, including electrochemical [Navadeepthy et al., 2020; Sapner et al., 2021; Faria et al., 2020], chromatography [Cotrut et al., 2016; Zhu et al., 2020], chemiluminescence [Wang et al., 2021; Zhu et al., 2016], enzyme-linked immunosorbent assay (ELISA) [Xie et al., 2020], fluorescence [Zhu et al., 2018; Meng et al., 2017] and colorimetric [Navadeepthy et al., 2020; Shu et al., 2020] have been well studied and established. Bio-sensing platforms have a broad range of technological array and have been explored to detect various small biomolecules, tumor markers, AA level, etc. [Wu et al., 2019; Zhang et al., 2017; Liu et al., 2013; Wu et al., 2017; Chen et al., 2019]. Among them, the colorimetric technique has positioned itself as an excellent method to expedite simplicity, quick, cost-effective, and visual detection [He et al., 2020; Ojha et al., 2020; Singh et al., 2021; Ojha et al., 2021; Vinita et al., 2018]. The colorimetric method is based on the chromogenic substrate, which produces color on oxidation under the effect of the enzymes. Therefore, the chromogenic substrate or reagents selection is a key point to manifest the colorimetric performance and effective detection of color transformation [Zhang et al., 2013]. Natural

enzymes are particularly ultra-sensitive in their working environments. If a bit of change occurs in their environmental conditions (pH, pressure, and temperature), they lose their catalytic activities. Therefore, regular application of natural enzymes realizes a group of difficulties and creates a significant challenge in the medical assay for performing enzyme-dependent reactions or processes [Chaibakhsh et al., 2019]. To counter such situations, researchers started developing some new materials that can show enzyme-like activity [Chaibakhsh et al., 2019]. Based on the catalytic concept, the high surface area and reaction centers are the main factors that shift the equilibrium toward their completion. Since the nanostructure has a high surface area and unique properties, nano-science provides a unique platform for integrating the desired artificial enzymes (also called nanozyme, nanoenzyme). With the development of nanotechnology, several nanomaterials, including transition metals [Ojha et al., 2020; Navadeepthy et al., 2017; Vinita et al., 2018; Asati et al., 2009], noble metals [Xi et al., 2021; Li et al., 2021], polymers [Oh et al., 2020; Zhang et al., 2021], carbons material [Wang et al., 2018] are developed and have been reported for mimic or colorimetric sensing purposes. Artificial enzymes having large surface areas are easy to store and employ. In addition, they can adopt harsh circumstances for denaturation, high substrate concentration, and low cost, and therefore, getting prime attention as an alternative to the natural enzymes [Ray et al., 2020; Jiang et al., 2019].

There are four types of nanozyme: oxidase, peroxidase, catalase, and superoxidase have been notified with their advantage and disadvantage. Much research literature has been reported so far for the detection of AA via oxidase and peroxidase activity. According to the reaction mechanism, the oxidase nanozyme is denoted as a better mean than the peroxidase because of the absence of corrosive H_2O_2 [Ojha et al., 2020]. Even though very little literature has been available on oxidase nanozyme for AA detection.

Thus, there is a high demand for sustainable, green, and efficient oxidase nanozyme for AA recognition. Since colorimetric detection of bio-molecules is based on electronic transfer processes and co-related with substrate surface area, porosity, and heteroatom in the lattice [Liang et al., 2019; Hou et al., 2019; Gurmessa et al., 2021]. Since porous 2D carbon bears a vast surface area and unique electronic structures; therefore, it can play an exciting role for the artificial enzyme. Presently, bio-waste-derived 2D carbon nanomaterials are acquiring much more attention in various recommended technological projects [Engelberth et al., 2021; Culebras et al., 2021], e.g., supercapacitor [Biswal et al., 2013; Verma et al., 2020; Ramirez-Castro et al., 2016], batteries [Yokokura et al., 2020], and adsorbents [Sabzehmeidani et al., 2021], etc. Despite this, some work has been published on the carbon-based substrate for mimetic purposes, but still, there is a need for more explorations.

In this work, we have derived N, O doped highly porous 2D carbon (BET surface area is 781 m^2g^{-1}) from a bio-waste Eichhornia Crassipes plant using a carbonization technique under an inert environment. Eichhornia Crassipes (locally called jalkumbhi) is an unwanted aquatic herb harming aquatic agriculture, fisheries, and water transportations. To improve the marine agricultural-based economy, much manpower works is consumed unnecessarily for netting such herbs and dumping around the water pounds and pools, causing environmental contaminations. Thus, some scientific approaches are needed to convert this bio-waste herb into a valuable material. Since Eichhornia Crassipes have massive moisture (~9.95), volatile matter (~56.30), fixed carbon (~17.40), and ash content (wt 16.35%), respectively. Water and volatile matter content probably act as self-activating means and provide high surface 2D carbon [Verma et al., 2020]. Motivated by the above facts, Eichhornia Crassipes has been used as a source for developing porous 2D carbon materials in this work which satisfied both techno- as well as socio-economical

features. The structural parameters of carbon material are characterized using Fourier transform Infrared spectroscopy (FTIR), X-ray diffraction (XRD), and X-ray photoluminescence spectroscopy (XPS). The surface morphology of materials was analyzed under a field emission scanning electron microscopy (FESEM) and transmission electron microscopy (TEM). The presented 2D carbon material shows an efficient affinity towards chromogenic substrate 3,3′,5,5′-tetramethylbenzidine (TMB), forming a characteristic oxidized blue color product. AA delivers concentration-dependent inhibition property over the 2D carbon oxidase activity and results in a decrease in color intensity. We have developed a colorimetric method for sensing AA based on this principle, producing a color contrast with its different concentrations. The technique is further explored to detect AA in actual samples (orange, lemon, grapes juice, and human serum) with a good recovery percentage.

4.2 Materials and Methods

4.2.1 Chemicals and Reagents

3,3',5,5'-tetramethylbenzidine (TMB), L-Ascorbic acid (AA), Hydrochloric acid (HCl), Hydrofluoric acid (H.F.), Copper(II) chloride ($CuCl_2$), Calcium chloride ($CaCl_2$), Potassium chloride (KCl), Citric acid, Glucose, Glutathione (GSH), Sodium acetate and glacial acetic acid were purchased from Sigma Aldrich. N-Ethylmaleimide (NEM, 98%) was purchased from Avra. All solutions were prepared in Milli-Q water (resistivity=18.0 MΩ, pH=7) during experiments. The human serum samples for the AA determination and recovery study were collected from the University hospital "the Institute of Medical Sciences, Banaras Hindu University" (courtesy Prof. D. Dash, IMS, BHU, Varanasi).

4.2.2 Characterization techniques

TEM micrographs of drop cast 2D carbon suspension in water were investigated on FEI, at an accelerating voltage of 200 kV on TECHNAI G^2 20 TWIN (Czech Republic) TEM instrument. Absorption spectra of 2D carbon mimetic activity and colorimetric assay have been done on a Biotek spectrophotometer (Epoch 2, USA). FT-IR analysis was carried out in the spectral range of 450-4000 cm^{-1} with a Thermo Scientific Nicolet 6700 FTIR spectrometer. X-ray photoelectron spectroscopy (XPS) was recorded on Kratos analytical instrument (Shimadzu, Amicus XPS, U.K.) equipped with MgKα (λ=1.254 Å) radiation. Rigaku miniflex 600 X-ray diffractometer with Cu Kα1 radiation (λ = 1.54056 Å was used for X-ray powder diffraction measurement of the prepared 2D carbon. The surface property of the material was investigated from Nova Nano SEM-450, FEI, the USA, and NTEGRA Prima, NT-MDT scanning probe microscope. For testing the method in an actual sample, oranges, lemons, and grapes have been bought from Varanasi supermarket.

4.2.3 Synthesis of porous carbon

The oxidase mimics porous 2D carbon has been synthesized using our previous protocols as reported [Verma et al., 2020]. In brief, Eichhornia Crassipes leaves were washed thoroughly after collection in running water and dried in the oven at 80^oC. Dried leaves have been deformed into fine powder form using a mortar pestle. Thus obtained powder was allowed for carbonization at 800^oC under inert N_2 conditions followed by an acid-base-water washing process. The carbon obtained has been stored at R.T. for further application.

4.3 Results and Discussions

4.3.1 Structural analysis

Since 2D carbons have porous architecture and heteroatom-doped sp^2 and sp^3 hybridized atoms, which is a fundamental point for any activated carbon. In this work, XRD, FTIR, and XPS techniques have been used to confirm successful material synthesis. The obtained results are very similar to our earlier work [Verma et al., 2020]. Figure 4.2 (a) shows FTIR of 2D carbon exhibiting a vibration band corresponding to a hydroxyl group, C=C/C-C stretching vibrations, and advocates the occurrence of the sp^2-hybridized graphitic system. A broadband (1000-1100 cm^{-1}) has been observed, indicating the C-O functionalities existence. Further, the XRD of such 2D carbon shown in Figure 4.2 (b), reflects two characteristic peaks as one broad peak around 2θ ~25° consequent to (002) plane, and the second peak at 2θ ~43°, which is committed for (100) plane. Such XRD data (broadening spectra) reveals that the prepared carbonic material is amorphous.

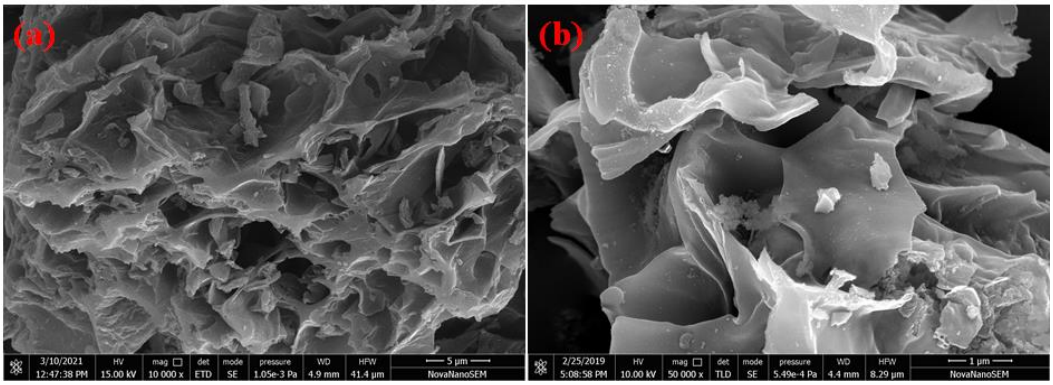

Figure 4.1 SEM image of 2D carbon (a) at 5μm scale, (b) at 1μm Scale

In order to understand the surface architecture of 2D carbon, TEM and SEM image investigations are performed (as shown in Figure 4.2 (c,d) and Figure 4.1 (a,b)), which disclose that the as-synthesized 2D carbon has a typical porous arrangement.

As presented in Figure 4.2 (c), the TEM image indicates that reported 2D carbon is made up of very tiny particles. Further, at high resolution, the HRTEM image, as shown in Figure 4.2 (d), reflects some prototype fringe which suggests that the 2D carbon construction is not fully amorphous but a few crystalline domains also in their matrix. This observation could be correlated to the presence of some sp^3 hybridized centers and heteroatom. Additional insurance about contamination-free 2D carbon, mapping (Figure 4.2 (e-h)) and EDX (*see* in Figure 4.2 (i)) is performed, which is further supported by the XPS observation [Verma et al., 2020] (also can be seen in Figure 4.3) vice-versa. The mapping shows that heteroatoms like N and O are distributed homogenously throughout the carbon matrix (*see* Figure 4.2 (e-h)). In the sum of these consequences, like the heteroatom, porous structure, and high surface area, the synthesized 2D carbon can be utilized as a fascinating mimetic substrate for establishing biosensors with high performances, which is explored very well in the next paragraph as colorimetric detection of AA.

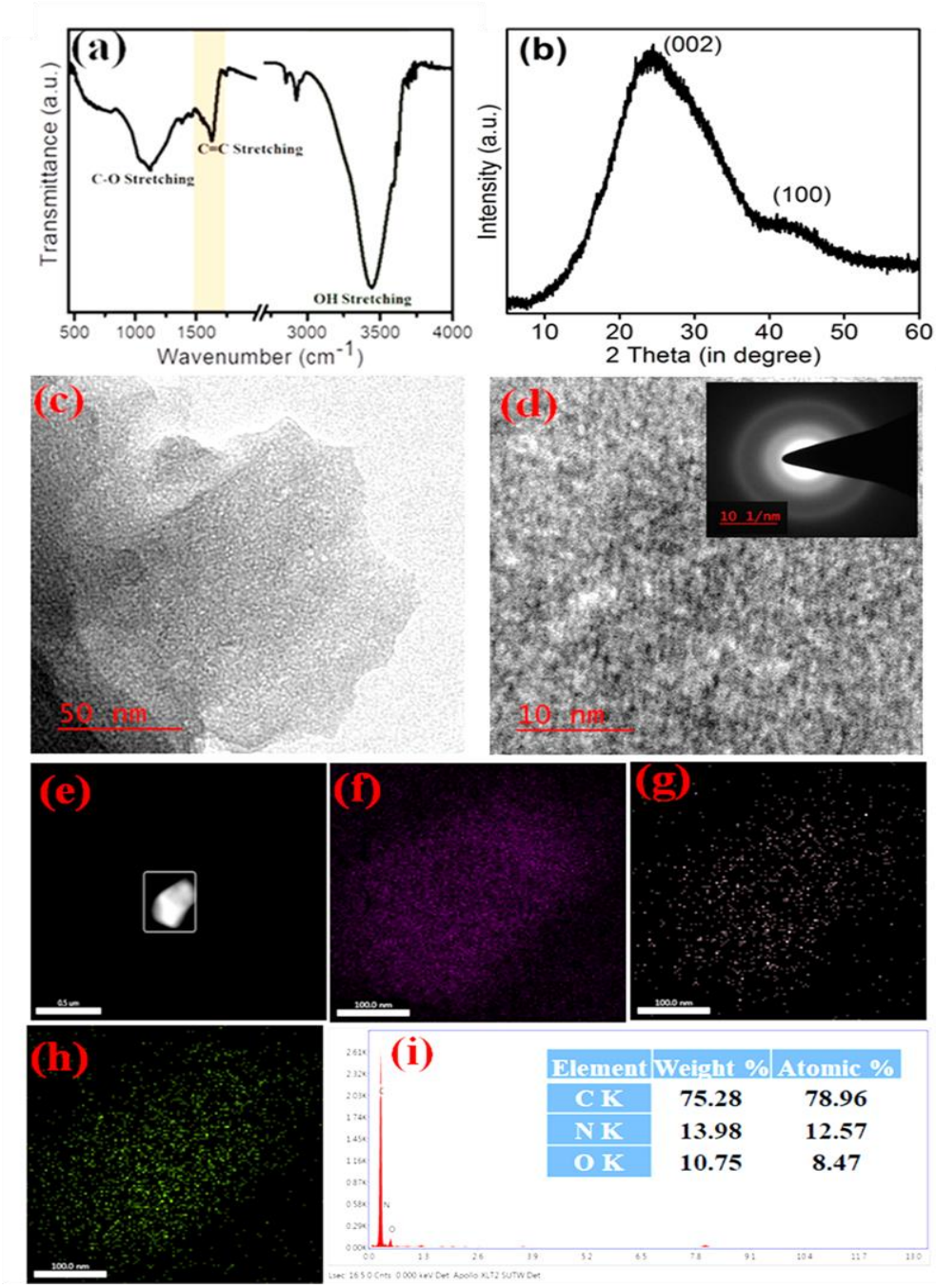

Figure 4.2 Characterization of 2D carbon. (a) FTIR spectrum, (b) XRD, (c) TEM image at 50 nm scale, (d) at 10 nm scale (Inset shows SAED pattern), (e) HAADF image area for mapping, (f) mapping image corresponding to C, (g) N, (h), O respectively.

The XPS survey spectrum study of 2D carbon, as represented in Figure 4.3 (a), shows three consequent peaks of C, N, and O elements. Further, deconvolution XPS data, the C1s peak of the 2D carbon (*see* Figure 4.3 (b)) is disassembled into the following three peaks as 284.9eV, 286.3eV, and 288.7eV related to the C-C-C, C-N/C-O and O-C=O bonds, respectively.

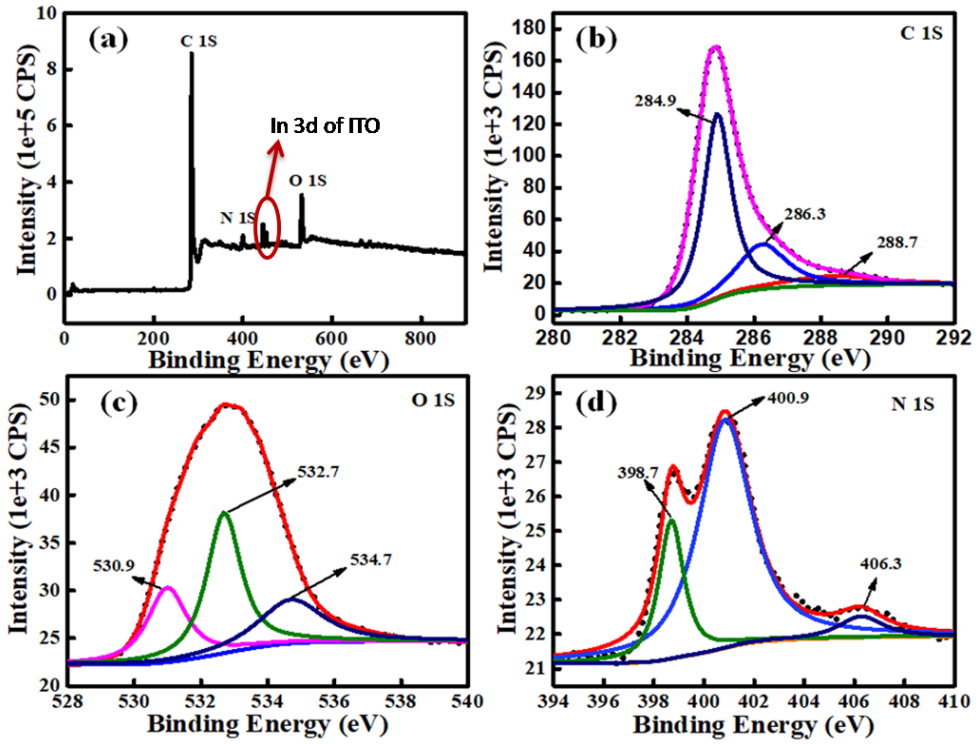

Figure 4.3 XPS study of 2D carbon (a) XPS survey spectrum, (b) Deconvoluted XPS spectra for C, (b) O, (c) N respectively. (Note-Here, ITO was used as substrate for XPS measurement, for which the peak appeared around (~450 eV) due to Indium element (In 3d)).

Further, the O1s deconvoluted spectrum (*see* in Figure 4.3 (c) exhibits three different oxygen moieties at 530.9eV, 532.7eV and 534.7eV for C-O-C of carboxyl groups, C=O and chemisorbed O_2, respectively. Finally, Figure 4.3 (d) shows the N1s peak disassembled into three sub-peaks at 398.7eV for imine nitrogen, at 400.9eV for pyrrolic, and 406.3eV for quaternary nitrogen. These data confirmed that the reported 2D carbon

has only C, N, and O elements as its constructing component and is free from contaminating features.

4.3.2 Oxidase mimetic activity of 2D carbon and AA inhibition

For H_2O_2-free colorimetric sensing of AA, the development of an oxidase-like nanozyme is an essential call for the researcher. Ensuing this, we have presented a sustainable 2D carbon material derived from bio-waste, which grasped an excellent oxidase mimetic activity in the presence of dissolved O_2. To investigate the oxidase property of 2D carbon material, absorption spectra of TMB were recorded in the absence of 2D carbon (*see* Figure 4.4 curve (a) and in the presence of 2D carbon (*see* Figure 4.4 curve (b)). The absorption spectra are shown in Figure 4.4 curve (a), suggesting that alone TMB aqueous solution is colorless due to the non-involvement of any charge transfer reaction. Although upon the addition of 2D carbon into the TMB aqueous solution, a strong absorption peak appeared at 652 nm (Figure 4.4 curve (b)). This peak occurrence at 652 nm is crystal-clear proof of a charge-transfer complex (CTC) between oxidized and unoxidized TMB. TMB molecules get oxidized with the help of added 2D carbon due to oxidase activity. Further, on the addition of AA into the reaction mixture of TMB+2D carbon, the absorption intensity of the 652 nm band gets diminished (*see* Figure 4.4 curve(c)). It validates the inhibition of the oxidase activity of 2D carbon. Lastly, the stop solution, H_2SO_4 was added, the absorption band at 652 nm corresponds to CTC gets diminished, and a new peak is generated at λmax = 450 nm as shown in Figure 4.4 curve (d). (A detailed discussion is provided in the later section, 4.3.5).

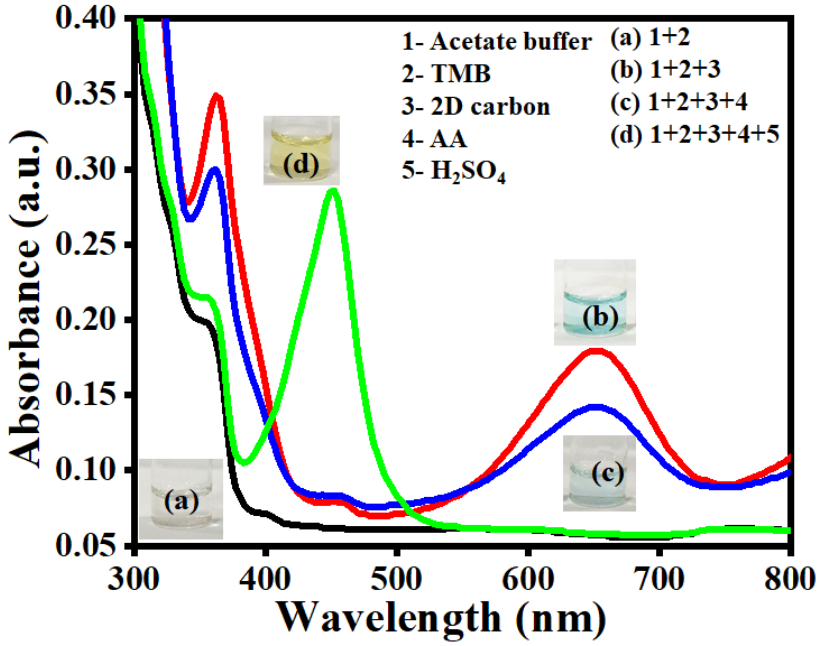

Figure 4.4 Absorption spectra for the oxidase activity of 2D carbon and inhibition property of AA

4.3.3 Role of Material and optimization towards oxidase

Since the colorimetric sensing response of the nanozyme is concentration-dependent; therefore, 2D carbon material concentration optimization is compulsory. For the test of variation in oxidase activity of 2D carbon towards TMB, a range of concentrations between 0.1 to 1 mg/ mL of 2D carbon has been applied. During the experiments, absorbance at 652 nm was recorded after an incubation period of 15 minutes, as shown in Figure 4.5. The absorbance result verifies in an approximately linear manner, and the response suggests that the saturation level happens after 0.8 mg/L. Based on this observation, the optimum concentration of 2D carbon e.g., 0.8 mg/mL has been chosen to perform further experiments. In this way, even at a low concentration of 2D carbon (i.e., 0.08 %), we are getting an excellent catalytic response.

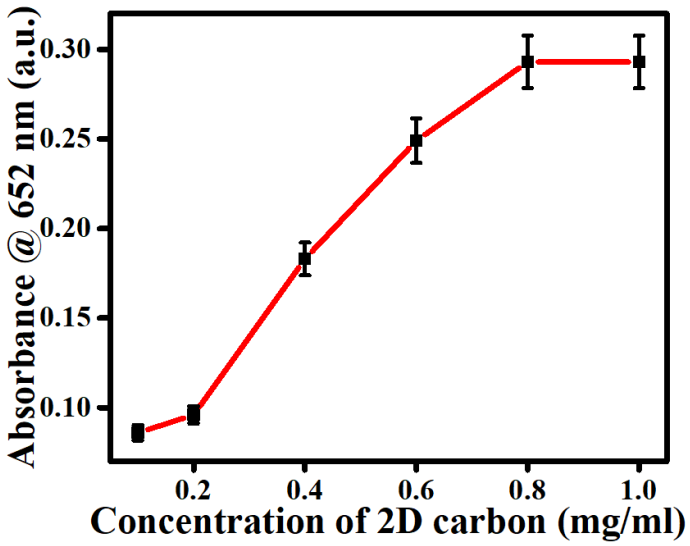

Figure 4.5 Endpoint spectrum for 2D carbon optimization.

4.3.4 TMB optimization and its Line weaver Burk plot

In order to investigate the nature of nanozyme kinetics, the oxidase activity has been studied under different TMB concentrations from 100 µM to 1000 µM. In this, the absorbance at 652 nm has been recorded under the pH=4 (which was adjusted by adding the acetate buffer). Figure 4.6 (a) depicts the absorbance plot at 652 nm *vs.* TMB concentration, indicating a saturation point after 800 µM. This data shows that intensity is directly proportional to the TMB concentration, but after 800 µM of TMB, peak intensity is almost constant. Figure 4.6 (b) shows the Lineweaver Burk plot of the 2D carbon nanozyme having an R-Square value of 0.99, which indicates a good linear response. Beer Lambert's law has been utilized to calculate the initial reaction rate using Eq. 4.1.

$$A = \varepsilon bc \quad \text{……..……..……..(Eq 4.1)}$$

where c is solution concentration, A represents absorbance, and b represents the thickness of the solution or path length. ε is the molar absorptivity coefficient having a value of 39,000 M^{-1} cm^{-1}. The Lineweaver-Burk plot for nanozyme catalysis reaction is plotted against reciprocal velocity and TMB concentration reciprocal. Michaelis–Menten

constant (Km) value for the 2D carbon as nanozyme has been calculated from the Lineweaver-Burk plot. The corresponding values of k_m are 0.121 mM, and V_{max} is 5.3 μM. The lower value of km of the proposed 2D carbon-based nanozyme shows a stronger affinity between the nanozyme and TMB substrate, resulting in a more efficient catalytic property of 2D carbon. This relationship is because this 2D carbon has a high surface area (781 m^2g^{-1}), giving more exposure for chromogenic substrate interactions and enhanced molecular interaction and electron transfer. For validating our appeal of the significance of the reported 2D carbon-based nanozyme, a comparison table has been made with other carbon-based materials and natural enzymes showing superior catalytic properties of 2D carbon (see table 4.1).

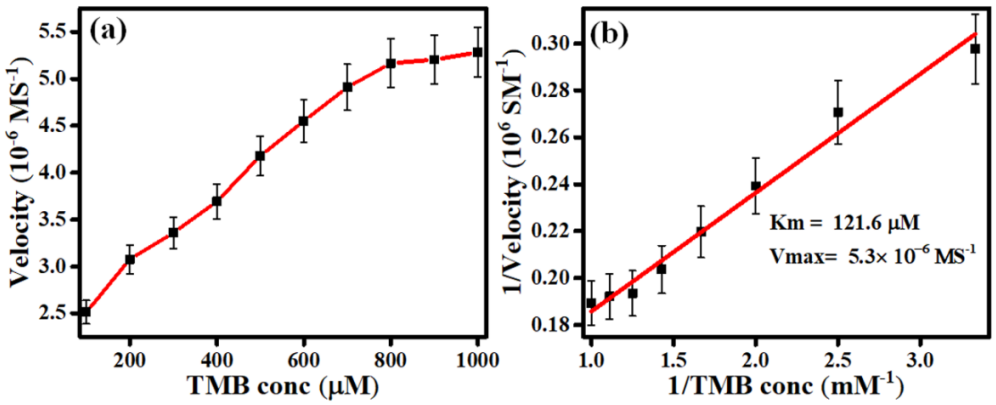

Figure 4.6 Steady-state kinetic assay of 2D carbon as nanozyme. (a) the variation of enzyme velocity with TMB concentration, (b) Lineweaver Burk plot.

Table 4.1: Comparison of catalytic property of 2D carbon with other nanozymes.

S. No.	Catalyst	Substrate	K_m (mM)	V_{max} (MS^{-1})	Reference
1	2D carbon	TMB	0.122	5.3 x 10^{-6}	This work
2	C-dots	TMB	0.039	3.61 x 10^{-8}	[Shi et al., 2011]
3	HRP	TMB	0.434	10 x 10^{-8}	[Chen et al., 2014]
4	N-GQDs	TMB	11.19	0.38 x 10^{-8}	[Lin et al., 2015]
5	Graphene-AuNPs	TMB	0.38	18.30 x 10^{-8}	[Chen et al., 2014]

4.3.5 Principle of colorimetric detection of AA

Josephy et.al. (1982) has been well established the oxidation phenomenon of TMB in the presence of a catalyst using optical and EPR spectroscopy [Josephy et al., 1982]. On behalf of this, we have demonstrated the reaction progress of oxidation of the TMB molecule to diimine (*see* Figure 4.7 Since TMB, in its reduced form, absorbs electromagnetic radiation around λ_{max}=285 nm region, the solution of TMB has no color. However, in the existence of dissolved oxygen and an oxidase nanozyme, the solution of TMB turned blue color. This is because a cation-free radical is generated, forming a CTC with unoxidized TMB, giving a blue color product with absorbance peaks at λ_{max}= 370 and 652 nm (*see* Figure 4.7 (i)). The radical cation is less stable and in rapid equilibrium with CTC. Upon the addition of stop solution (H_2SO_4) (*see* Figure 4.7 (ii)), which lowers the pH from 4 to around 1 and thereby the enzymatic reaction becomes terminating. The lowering of pH causes the shift in equilibrium from CTC to its radical cation favoring the formation of a yellow diimine product with λ_{max}= 450 nm and significantly higher molar absorptivity [Bally et al., 1989].

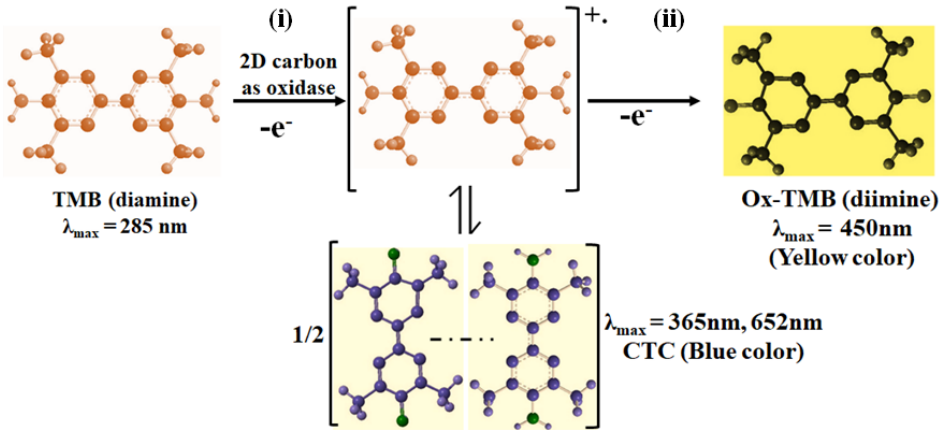

Figure 4.7 Schematic representation of oxidation of TMB.

After understanding the oxidation reaction of TMB, we are now in a position to elucidate the nonozyme activity of the proposed 2D carbon. 2D carbon has been

synthesized from Eichhornia Crassipes leaves by the carbonization technique as shown in Figure 4.8. Since nanozyme mimicking oxidase functions as a catalyst that accelerates TMB oxidation by mediating the electron transfer from TMB to dissolved oxygen [Qin et al., 2014; Han et al., 2022] and better substitute to the peroxidase because of the absence of corrosive H_2O_2 [Ojha et al., 2020]. So our interest is focused on the investigation of oxidase-like nanozyme. The offered 2D carbon possesses excellent surface area with profound oxidase activity corresponding to chromogenic substrate TMB. Due to the large surface area, more TMB and O_2 molecules get adsorbed over the 2D carbon. Due to such proximity, the reacting molecules become closer together, facilitating electronic or redox reactions. There is a net transfer of electrons from TMB to the catalyst (2D carbon), forming oxidized TMB; further oxygen receives the electron from the catalyst and gets reduced. 2D carbon bears another advantage as it has O, N heteroatoms in, making H-bonding and acting to better mimic activity. AA is an antioxidant and has competitive inhibition properties concerning the oxidase activity of 2D carbon towards TMB. Therefore, with the addition of AA, the oxidation of TMB is inhibited, resulting in the lowering of peak intensity at 450 nm and producing yellow color contrasts.

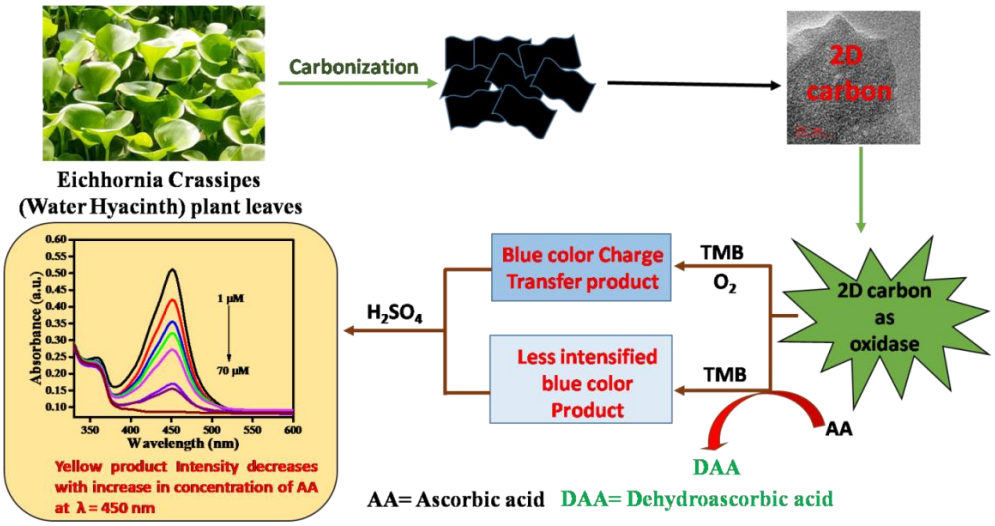

Figure 4.8 Schematic representation of the principle for colorimetric detection of AA

A linear response is achieved for absorbance at 450 nm for different AA concentrations. This oxidation reaction between 2D carbon and TMB is a corrosive H_2O_2-free process and has excellent sensitivity, stability, and reproducibility, which is the significance of the reported 2D carbon material.

4.3.6 pH and Temperature Parameters

The catalytic properties of enzymes are susceptible to different parameters, such as pH and temperature. So, optimizing these parameters is crucial for developing an efficient sensor with better accuracy and precision. For temperature optimization, the experiment of oxidase activity has been tested at different temperatures ranging from 10 to 50 ^{0}C. Figure 4.9 (a) shows that 2D carbon exhibits good mimetic activity over a broad temperature spectrum with maximum activity at 20 ^{0}C. Further, to optimize pH, the oxidase activity experiment has been tested in buffer solutions of varying pH (2, 3, 4, 5, 6, 7), as shown in Figure 4.9 (b). In Figure 4.9 (b), it has been found that 2D carbon has maximum activity at pH 4, which is consistent with earlier reports [Ojha et al., 2020]. Such results show the resistance of 2D carbon catalytic property to pH and temperature compared to the natural enzyme and suggest the better stability and efficiency of the developed nanozyme.

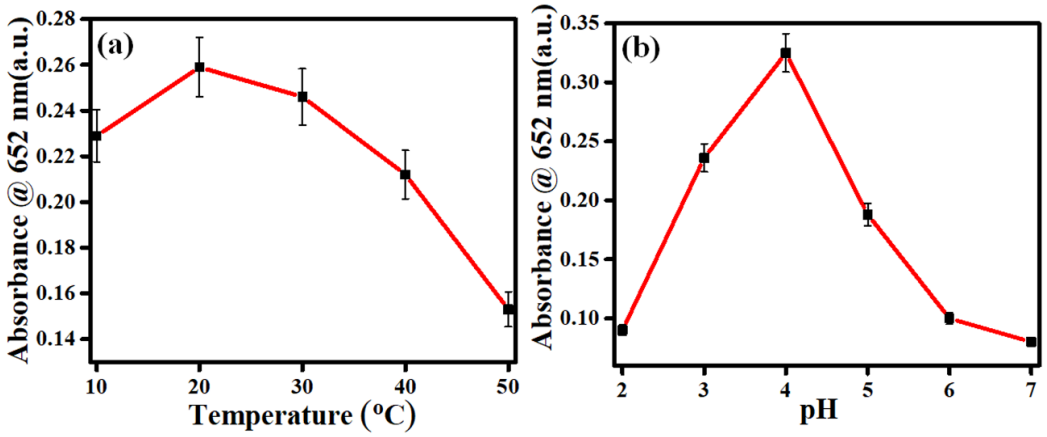

Figure 4.9 Spectrum for the optimization of the parameters for nanozyme. (a) Temperature, (b) pH

4.3.7 Sensing

Under all optimized conditions of temperature, pH, material concentration, and TMB, the developed methods have been explored for the sensing of AA. Since AA shows inhibition properties over the oxidase activity of 2D carbon and is concentration-dependent. 2D carbon induced oxidation reaction of TMB and displays blue color as charge transfer complex formed. This blue color transforms to yellow upon adding the stop solution and gives a characteristic absorbance peak at 450 nm. The addition of AA gives a color contrast with its different concentrations. Figure 4.10 (a) represents the sensing of AA and shows the developed sensor shows good linearity in the range of 1 to 70 μM with a regression coefficient of 0.99. Figure 4.10 (b) shows the linear calibration plot, which has been plotted, taking the average after ten replicates. The developed sensor shows good linearity with a detection limit of 0.26μM calculated using the formula LOD= 3*standard deviation of blank/slope of calibration plot.

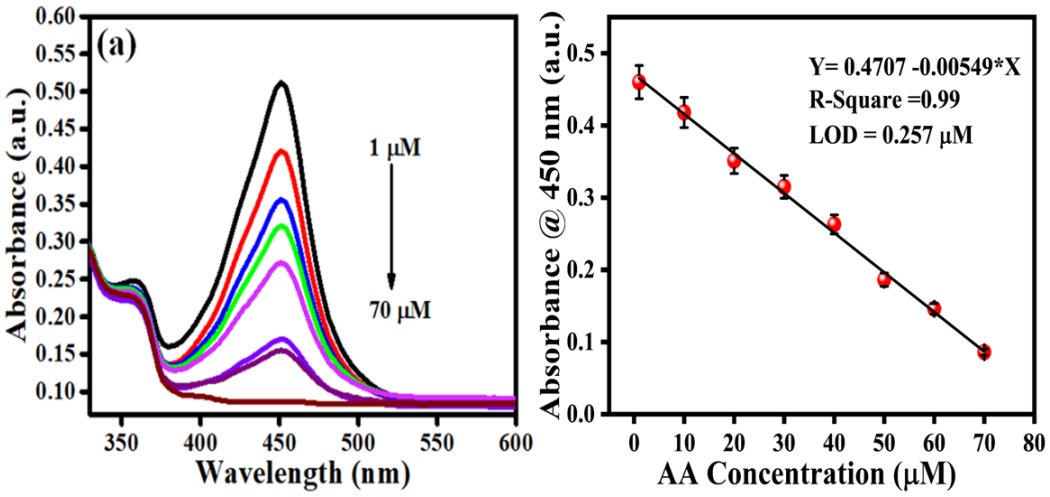

Figure 4.10 (a) UV-Vis absorption spectra for AA sensing (1 to 70 μM). (b) Endpoint calibration plot at 450 nm.

4.3.8 Reproducibility and cycle stability

In order to elucidate the reproducibility of the developed sensor, we have repeated the experiment several times using freshly prepared solutions for all components, as described in Figure 4.11 (a). It can be inferred from the result that the sensor's relative activity was similar over ten days with inefficient differences. Further, the recyclability test of the nanozyme has been tested by recovering it after the test through centrifugation at 8000 rpm for 10 min. For this purpose, 30 min incubation time has been reserved. As can be observed in Figure 4.11 (b), the relative activity of the nanozyme shows good cycle stability over six cycles with more than 94 %. This minor reduction may be due to the sample loss during centrifugal treatment [Jin et al., 2019].

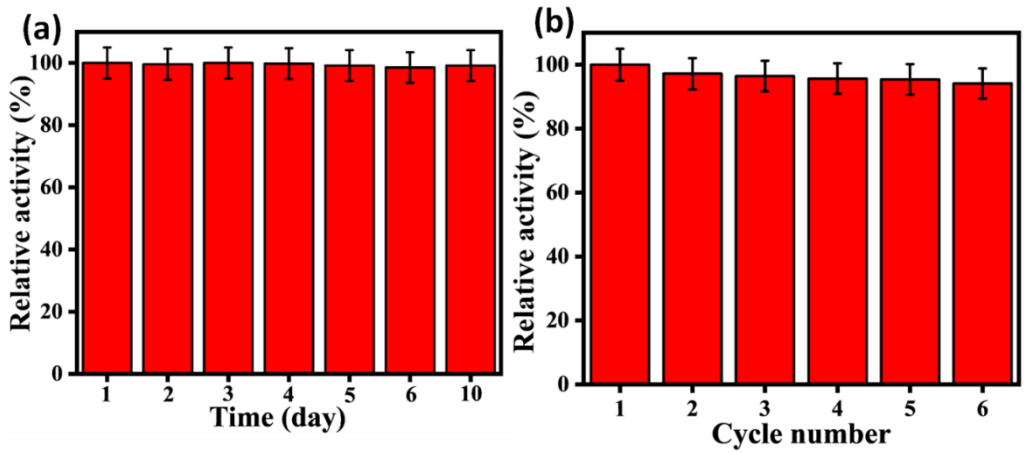

Figure 4.11 (a) Reproducibility study over different days, (b) cycle stability of catalytic activity of 2D carbon

4.3.9 Interference Study

For any sensor, specificity, and selectivity are essential parameters. Before commercialization, an interference study is necessary to ensure the selectivity of sensors toward the targeted molecules. The real sample can encounter several molecules, which may interfere with the sample analysis and misleads the data

interpretations. In this work, the method has been examined with various interferences encountered like glucose, citric acid, glutathione, Cu^{2+}, Ca^{2+}, K^{+}, and Cl^{-}, taking their concentration ten times high to the AA Since GSH has a reductive nature like AA, that gives a very similar response to the reported method. The comparative responses of the interferences, as mentioned above with AA, are shown in Figure 4.12. Thus, there is a critical step for the investigation of the GSH effect. To understand, similar experiments for the oxidase activity have been performed in the absence and presence of NEM. NEM is an alkylating compound commonly used to protect the thiols group (-S.H.) of GSH. Thereby, we negotiate the effect of GSH in our AA sensing [Huang et al., 2018; Zhu et al., 2021]. The histogram of Figure 4.12 depicts that the present method is particular for AA, and can be effectively applied as a selective technique for sensing AA in actual samples.

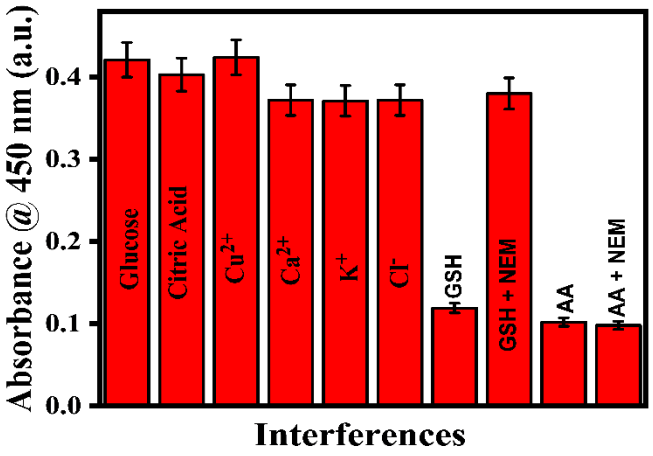

Figure 4.12 Interference study of AA in the presence of Glucose, Citric acid, Cu^{2+}, Ca^{2+}, K^{+}, Cl^{-}, and GSH (in the absence and presence of NEM)

4.3.10 Real sample analysis

Three different AA-rich fruits like oranges, lemon, and grapes, and human serum have been used for the objective sample analysis and tabulated as Tables 4.3 and 4.4. In order to do this, juices of oranges, lemons, and grapes have collected and centrifuged at 8000

rpm to get the extract. Consequently, each extract is diluted up to 50 folds (using buffer) and used for further experiments. The AA analysis has been performed by spiking different AA concentrations (10 and 20 μM) for each fruit extract, and the absorbance is recorded at λ_{max} 450 nm. By using the absorbance data, the concentration of AA has been calculated from the calibration plot, and their respective concentrations are given in Table 4.1. The observed result clearly shows the potential of our method with excellent recovery between 97 to 106 %. However, human serum (samples obtained from IMS-BHU Hospital) is diluted up to 10 folds using acetate buffer, and an experiment has been performed via spiking of different AA concentrations (20 and 40 μM). The observed result clearly shows the potential of our method with excellent recovery response between 93 to 103 % [*see* Table 4.4]. The Comparative data of the projected colorimetric method with the previously reported nanozyme are also tabulated in Table 4.2.

Table 4.2 Comparison table for the 2D carbon with other nanozymes

Material used	**Method**	**LOD (μM)**	**Linear range (μM)**	**Reference**
2D carbon	Colorimetry	0.26	1-70	This work
AuNPs	Colorimetry	0.3	1-15	[Zhang et al., 2012]
Cu/Ag/rGO	Colorimetry	3.6	1-30	[Darabdhara et al., 2017]
MIL-68/MIL-100	Colorimetry	6	30-85	[Zhang et al., 2014]
$CuCo_2O_4$ Microspheres	Colorimetry	0.57	1.00-10.00	[Han et al., 2021]
AgFKZSiW_{12}/PPy	Colorimetry	2.7	1 - 80	[Li et al., 2019]
CuFKZP$_2$$W_{18}$/PPy (15%)	Colorimetry	0.627	5-100	[Li et al., 2020]

Thus, the present technique based on 2D carbon nanozyme possesses good linearity and lower LOD. Therefore, we can say that Eichhornia Crassipes-derived 2D carbon-based colorimetric detection provides a reliable, highly sensitive, and convenient approach for detecting AA.

Table 4.3 Real sample analysis of AA in orange, lemon, and grapes extracts

50 times diluted juice	**Spiked Ascorbic acid (μM)**	**Found Ascorbic acid (μM)**	**Recovery**
Orange (33.46 μM)	0	33.46	100%
	10	43.56	100.2%
	20	52.38	97.9%
Lemon juice (24.44 μM)	0	24.44	100%
	10	34.76	100.9%
	20	43.16	97.1%
Grape (18.04 μM)	0	18.04	100%
	10	29.86	106%
	20	39.78	104.5%

Table 4.4 Sensing of AA in human serum

10 times diluted serum in buffer	**Spiked Ascorbic acid (μM)**	**Found Ascorbic acid (μM)**	**Recovery**
Human serum (21.3 μM)	0	21.18	100%
	20	42.54	103.2%
	40	57.36	93.5%

4.4 Conclusions

Herein, we present a bio-mass waste-derived 2D carbon-based sustainable, rapid, and efficient oxidase mimic for AA colorimetric detection from Eichhornia Crassipes. Such 2D carbon has a high surface area (781 m^2g^{-1}) with self-doped O, N heteroatom, which gives unique electronic or redox properties. The developed 2D carbon-based sensor shows excellent linear response (R-square = 0.99) over the range of 1 to 70 μM. The detection limit is found to be 0.26μM by introducing a sensitive platform for sensing the AA in real samples. Further, the reported oxidase 2D carbon-based sensor quantifies AA concentration in orange, lemon, grapes juice, and human serum with good recovery value. In conclusion, this work approaches a completely metal-free and efficient nanozyme based on Eichhornia Crassipes bio-waste. It presents a new avenue to design a sustainable mimetic substrate for ascorbic detection from bio-wastes.